The analysis of large scale atmospheric circulation which intensified the Baiu-front : a case study of "the extremely heavy rainfall in Japan, July 2006".

Yayoi Harada[1], Hiroaki Naoe[2]
[1]Japan Meteorological Agency
[2]Meteorological Research Institute

1. Introduction

Heavy rainfall with a daily accumulation of precipitation in excess of 300 mm has the potential to cause serious flooding and disasters. Such rainfall is frequently observed in Japan islands during the Baiu season. The Baiu season is defined in East Asia as the rainy period from early June to the middle of July.

In July 2006, the extremely heavy rainfall brought serious damages to the western and eastern regions of Japan. Total amount of precipitation broke the highest records, for example, 1281 mm (18 - 24 July) in Ebino city in the southern part of Kyushu and 701 mm (15 - 21 July) in Tamaki village in the central part of Japan, and so on. As a result, 28 deaths were reported by the Japanese Fire and Disaster Management Agency.

This can be seen in Fig.1, which shows the distributions of daily precipitation during the period of 15 - 24 July. As shown in Fig.1, apparently the distributions in the former period are different from those in the latter. On 17 - 18 July, the areas that exceeded 100 mm/day above are seen widely from Western Japan to eastern part of Japan. On the contrary, on 20 - 23 July, they are concentrated in Kyushu. This indicates that the precipitation systems in the former period of the heavy rainfall were different from those in the latter period. Hence, the period of the heavy rainfall can be divided into two periods; the former period is 15 - 19 July, and the latter 20 - 24 July). As we will see later, a strong Rossby wave packet propagated along the Asian jet and intensified the trough to the north of Japan. Thus, the purpose of this study is to analyze and distinguish the features of large scale atmospheric circulation as a circumstance of such extremely heavy rainfall. To clarify the details of this Rossby wave propagation, we conducted simple numerical experiment using the nonlinear barotropic model.

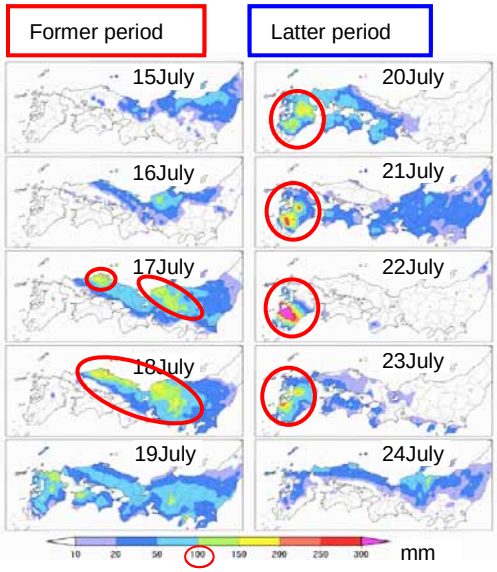

Fig.1 Distributions of daily precipitation from 15 to 24 July 2006.

In the present paper, data and the basic equation used in this study are presented in Section 2. In Section 3, observational results are shown. Section 4 describes the results of the numerical experiment. Summary and concluding remarks are presented in Section 5.

2. Data and Method

2.1 Datasets and analysis method

In this study, we used the 6-hourly reanalysis datasets produced through the Japanese 25-year Reanalysis (the JRA-25) Project and the Japan Meteorological Agency (JMA) Climate Data Assimilation System (JCDAS) (JRA/JCDAS hereafter) (Onogi et al., 2007). We also used the daily grid data of the US National Oceanic and Atmospheric Administration (NOAA) interpolated outgoing long-wave radiation (OLR).

Wave activity flux indicates a propagating packet of Rossby waves. It is calculated as described by Takaya and Nakamura (2001).

In order to confirm whether the tropical or extra-tropical convections work as a part of the source of Rossby

wave or not, the Rossby wave source (S') were calculated (Lu and Kim, 2004).

$$
\begin{aligned}
S' &= -\nabla\cdot\{(f+\overline{\zeta})V_{div}' + \zeta'\overline{V_{div}} + \zeta' V_{div}'\} \\
&= -(f+\overline{\zeta})D' - V_{div}'\cdot\nabla(f+\overline{\zeta}) \\
&\quad -\zeta'\overline{D} - \overline{V_{div}}\cdot\nabla\zeta' \\
&\quad -\zeta' D' - V_{div}'\cdot\nabla\zeta'
\end{aligned}
\tag{1}
$$

: where f, ζ, $Vdiv$ and D are Coriolis parameter, relative vorticity, divergent wind and divergence, respectively. Over-bars and primes indicate climatological mean and anomaly from climatological mean, respectively. The vorticity advection is the total of the second, forth and sixth term of the equation (1).

2.2 The nonlinear barotropic model

The basic equation used in our numerical model is a non-divergent vorticity equation:

$$
\begin{aligned}
&\frac{\partial\zeta'}{\partial t} + J(\psi_b,\zeta') + J(\psi',f+\zeta_b) + J(\psi',\zeta') \\
&\quad = F' - k_d\zeta' - \mu_d\nabla^4\zeta',
\end{aligned}
\tag{2}
$$

where f is the Coriolis parameter; Ψ_b and ζ_b are the stream function and relative vorticity of the basic flow, respectively; Ψ' and ζ' are perturbations of the stream function and relative vorticity from the basic flow, respectively; kd is a linear damping with a time scale of 14.7 days; μ_d is a biharmonic diffusion, and we set μ_d = $2.338\text{x}10^{16}$ m^4 s^{-1} (from Sardeshmukh and Hoskins, 1988). F' is intended as a local vorticity source and may be specified as $-fD$, where D is divergence.

$$
J(A,B) \equiv \frac{1}{a^2\cos\theta}\left(\frac{\partial A}{\partial\lambda}\frac{\partial B}{\partial\theta} - \frac{\partial A}{\partial\theta}\frac{\partial B}{\partial\lambda}\right)
\tag{3}
$$

where a is a radius of the earth, θ is latitude and λ is longitude. Equation (1) is numerically integrated using the spectral transform technique. A triangular truncation at wave number 42 is adopted in this study. The other details of the numerical model are described in Naoe and Matsuda, 1998.

3. Results and discussion

3.1 The features of atmospheric circulation

3.1.1 The activity of the Baiu front

Fig.2 shows water vapor flux anomalies at 925-hPa and vertical velocity at 500-hPa. Just before the former period of the heavy rain (Fig.2a), remarkable water vapor tranport towards the Baiu front are seen. In the former period, strong upward flows along the Baiu front are also seen. The Baiu period is defined from 31 May to 24 July every year from 1979 to 2005. The regional and 5-days averaged water vapor flux anomalies in the just before the rainfall are compared to the maximum values of 5-day and regional averaged water vapor flux anomalies during the Baiu period each year (Fig.3). It is found out that the value in just before the former period is the largest since 1979. The regional averaged vertical

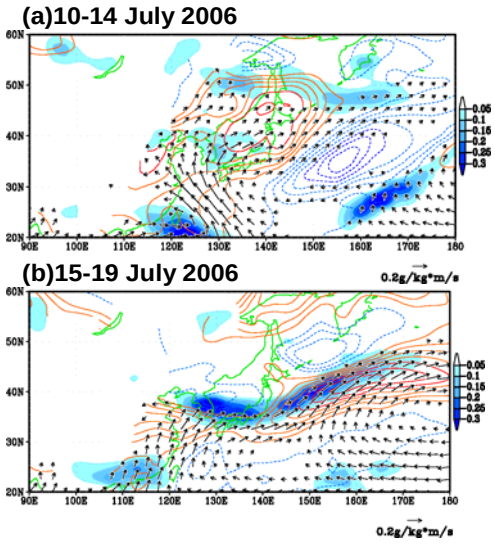

Fig.2 Anomalies of 5-day averaged 925-hPa equivalent potential temperature and water vapor flux and 500-hPavertical velocity. Shadings show 500-hPa vertical velocity anomalies (Pa s^{-1}). Contours show 925-hPa equivalent potential temperature anomalies (K) with an interval of 2K. Vectors show water vapor flux anomaly (g kg^{-1}*ms^{-1}).

velocity anomalies in the former period are also compared to the minimum values of 5-day and regional averaged vertical velocity anomalies during the Baiu period each year (Fig.4). It is also the lowest since 1979. This means the strongest upward flow existed in the former period. These features indicate the baiu front was unprecedentedly active in the former period.

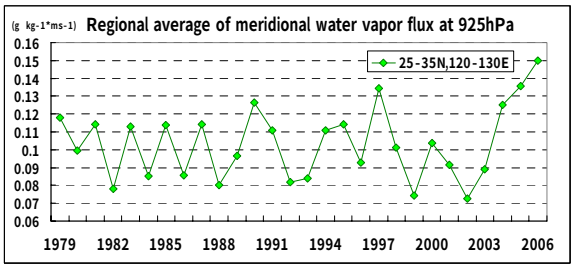

Fig.3 Time series of the maximum of regional averaged 925-hPa meridional water vapor flux during the Baiu period.

Each year's value shows the maximum of 5-day and regional averaged meridional water vapor flux from 31 May to 24 July. For 2006, the symbol shows the value on 10-14July.

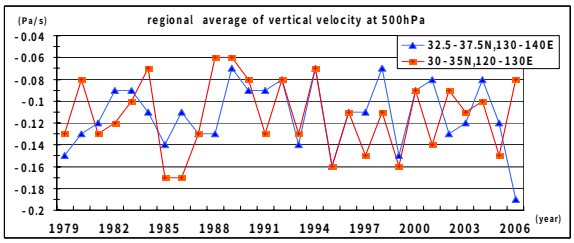

Fig.4 Time series of the minimum of regional averaged 500-hPa vertical velocity during the Baiu period.

Each year's value shows the minimum of 5-day and regional averaged vertical velocities from 31 May to 24 July. For 2006, the triangular symbol shows the value in the former period of the heavy rain and square symbol shows the value in the latter period, respectively. Unit in Pa/s.

Fig.5 shows 850-hPa wave activity flux and stream function anomaly and OLR anomaly averaged 11 - 15 July 2006. At that time, Typhoon BILIS was moving northwestward from the western Pacific to southern China. Rossby wave packets from Typhoon BILIS to anti-cyclone over Japan are clearly seen. This indicates the typhoon strengthened the high pressure over Japan and increased water vapor transport towards the Baiu front over the East China Sea.

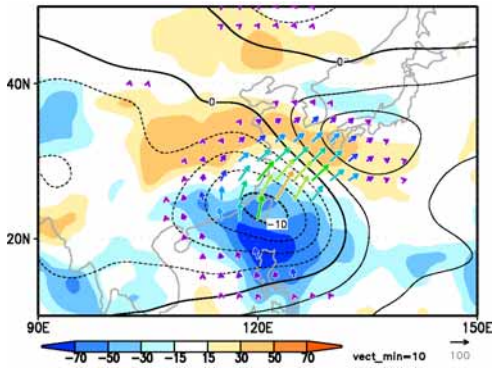

Fig.5 850-hPa wave activity flux and stream function anomaly and OLR anomaly averaged 11-15 July 2006.

Contours show stream function anomaly in an interval of $5x10^6$ m^2 s^{-1}. Shadings show OLR anomaly (Wm^{-2}). Vectors show wave activity flux (m^2 s^{-2}).

3.1.2 The condition of westerlies and Rossby wave packet propagations in July 2006

In this section, it is described that the features of westerlies and the Rossby wave propagation observed together with the heavy rainfall almost simultaneously. Fig.6 shows 250-hPa wind and anomalies averaged 2 - 16 July 2006. Strong wind anomalies are clearly seen around the Asian jet core. Weak wind anomalies are also seen to the north of the Asian jet core. That is to say, the wave guide was formed more sharply than its normal around the Asia jet. In addition, the weak wind anomalies in the higher latitudes indicate that if a Rossby wave packet propagates in this region, a breaking of Rossby wave is highly probable and isolated lower potential vorticity (hereafter low-Q) and higher potential vorticity (hereafter high-Q) are often formed. In fact, when the quasi-stationary Rossby wave packet propagated along the polar front jet in early July, the penetrations of Low-Q were often observed. High-Q was cut off by the breaking of the Rossby wave to the north of the Lake Balkhash (Fig.7a) and the inversion of potential vorticity over eastern Siberia occurred and persisted (Fig.7b). In such conditions, the quasi-stationary Rossby Wave propagated from Europe to Japan along the Asian jet

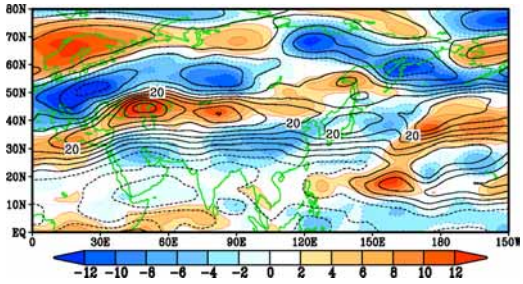

Fig.6 250-hPa wind and anomalies averaged 2-16 July 2006.

Unit in m s^{-1}.

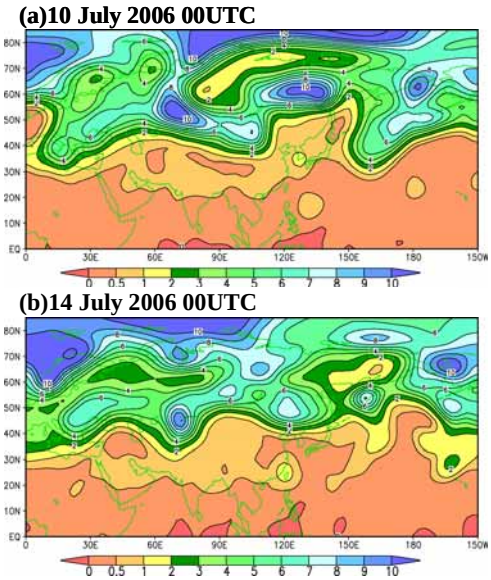

Fig.7 340K potential vorticity.
Unit in PVU (1PVU=10^{-6}m^{2}s^{-1}K kg^{-1}).

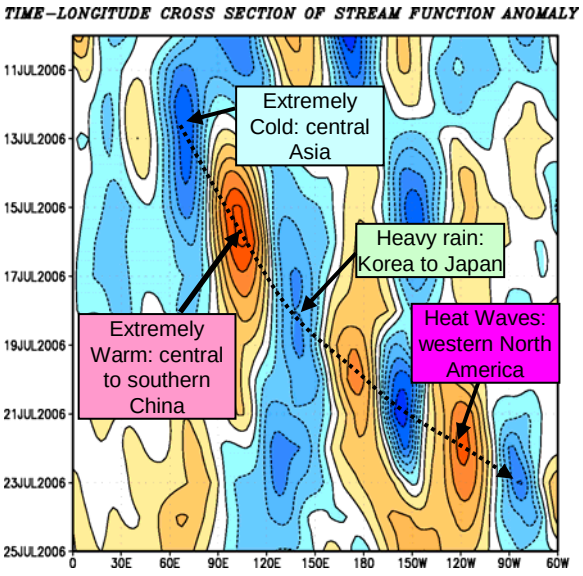

Fig.8 Time-longitude cross section of 250-hPa stream function anomaly averaged 40-50N.
Contours show stream function anomaly based on the climatological mean of 1979-2004 normal in an interval of 5x10^6 m^2 s^{-1}. Red and blue shadings show positive and negative anomaly, respectively. Dotted line indicates quasi-stationary Rossby wave propagation.

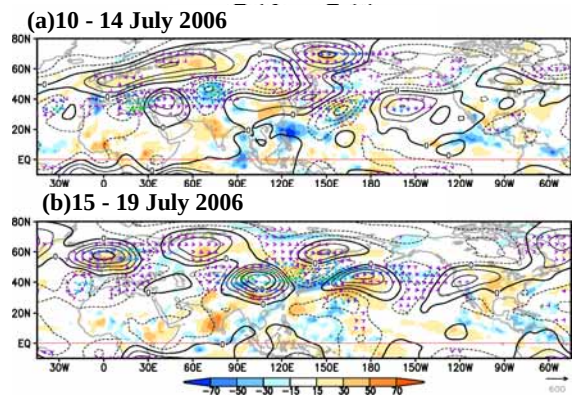

Fig.9 250-hPa wave activiy flux and stream function anomaly and OLR anomaly.
Contours show stream function anomaly based on the climatological mean of 1979-2004 normal in an interval of 5x10^6 m^2 s^{-1}. Shadings show OLR anomaly on the climatological mean of 1979-2004 normal (W m^{-2}). Vectors show wave activity flux(m^{2}s^{-2}).

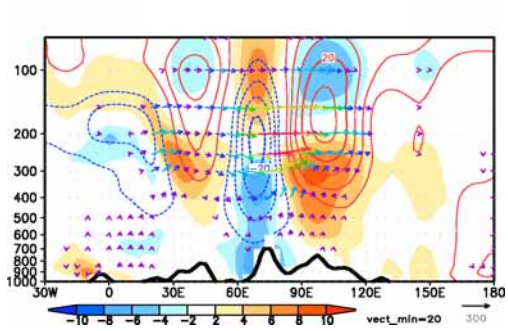

Fig.10 Height-longitude cross section of wave activity flux and stream function anomaly and temperature anomaly averaged 12 - 16 July 2006 along 40N.
Contours show stream function anomaly based on the climatological mean of 1979-2004 normal in an interval of 5x10^6 m^2 s^{-1}. Shadings show temperature anomaly on the climatological mean of 1979-2004 normal (℃). Vectors show wave activity flux (m^2 s^{-2}).

(Fig.8 and Fig.9). The activity of the Rossby wave in mid-July was the strongest since 1979 (not shown). It is clear that such strong Rossby wave caused the meandering of westerlies in East Asia. As shown in Fig.8, this Rossby wave propagation is associated with not only the heavy rainfall in Japan but the extremely hot and cold weather in other regions of the world. In addition, an eddy which had baroclinic wave structure developed around Lake Balkhash (Fig.10). It appears to have strengthened the Rossby wave along the Asian jet. Fig.11 shows 250-hPa Rossby wave sources averaged 11-20 July and indicates that the strong wave source existed around Lake Balkhash. Fig.12 shows total convective precipitation from 12 to 16 July 2006 (left) and 750-hPa convective heating rate averaged 12-16 July 2006 (right). These indicate there existed active convections around Lake Balkhash which were related to the development of the baloclinic eddy.

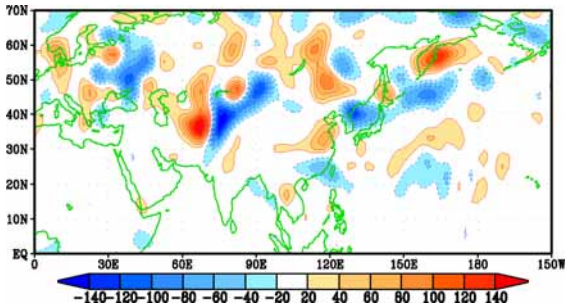

Fig.11 250-hPa Rossby wave source averaged 11-20 July 2006.
Shadings show Rossby wave source anomaly on the climatological mean of 1979 - 2004 normal. Blue and Red shadings show the generation of negative and positive vorticity respectively. Contour interval is 20 $x10^{-11}$ s^{-2}.

Table.1 Description of experimental design.

Vorticity Forcing 1(VF1)	
switch on	1st day
switch off	4th day
latitude	25.0 N
longitude	7.5E
size	Zonal Wave Number 8
amp.	0.15Ω (Ω = 7.292x10^{-5}/s)
Vorticity Forcing 2(VF2)	
switch on	2nd day
switch off	13th day
latitude	40.0N
longitude	67.5E
size	Zonal Wave Number 8
amp.	0.30Ω (Ω = 7.292x10^{-5}/s)
Vorticity Forcing 3(VF3)	
switch on	2nd day
switch off	13th day
latitude	42.5N
longitude	82.5E
size	Zonal Wave Number 8
amp.	-0.30Ω (Ω = 7.292x10^{-5}/s)
perturbation	
start day	2nd day
end day	4th day
latitude	45.0N
longitude	76.0E
size	Zonal Wave Number 8
amp.	-0.27x10^{6}

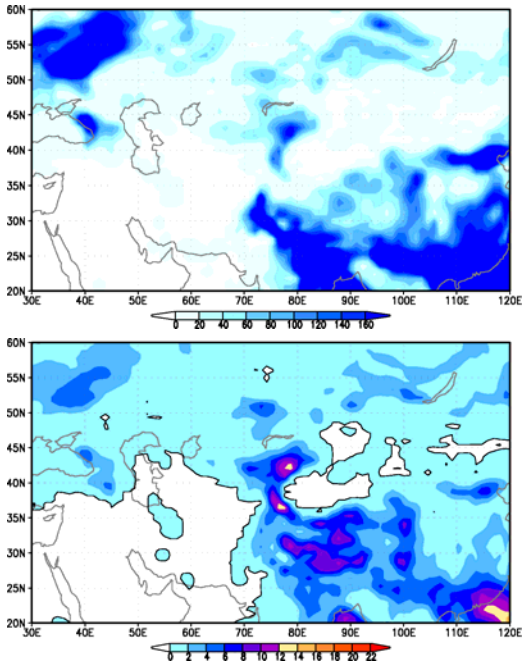

Fig.12 Total convective precipitation rate on 12-16 July 2006 (top) and 750-hPa convective heating rate averaged 12-16 July 2006 (bottom).
Unit in mm day^{-1} (top) and K day^{-1} (bottom), respectively.

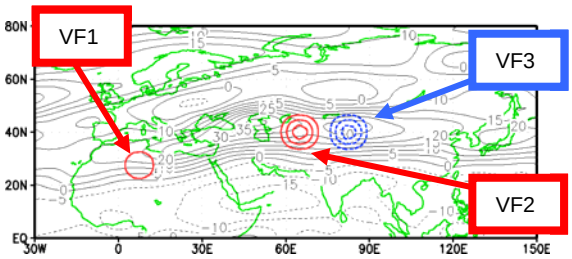

Fig.13 Idealized vorticity forcings
Contour interval is 5x10^{-6} (s^{-1}).

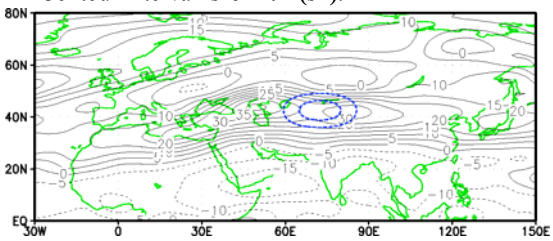

Fig.14 Idealized perturbation
Contour interval is 0.2x10^{6} (m^2 s^{-1}).

3.2 Simple numerical experiments

3.2.1 Experimental design

In this numerical experiment, the 15-day running mean of the 250-hPa wind data are used as the basic flow. The period of time-integration is from 9 - 25 July 2006. The three idealized steady forcing is used to examine the evolution of perturbation field in the realistic basic flow (Fig.13). One is centered at northern Africa (VF1). It was switched on at Day 2 and off at Day 4. The others were located to the south of Lake Balkhash (VF2 and VF3). Those were switched on at Day 3 and off at Day 10. Furthermore, we also used the idealized perturbation (IP) centered Lake Balkhash (Fig.14). The details are described in Table.1.

3.2.2 Results

Fig.15 shows the results of numerical experiments. The Rossby wave propagation from Eurasia to northern America is generally reproduced. In Exp.EX-ALL (Fig.15b), comparing to the analysis, we can see that the Rossby wave packet propagation over Eurasia and zonally elongated anti-cyclonic circulation over northern China were generally reproduced. In Exp-NOVF23 (Fig.15c), which is the result of the experiment without VF2 and VF3, the strong and zonally elongated anti-cyclonic circulation couldn't be reproduced. Considering these results, we were able to find out that the vorticity sources around Lake Balkhash were highly important for the realistic and strong Rossby wave packet propagation along the Asian jet.

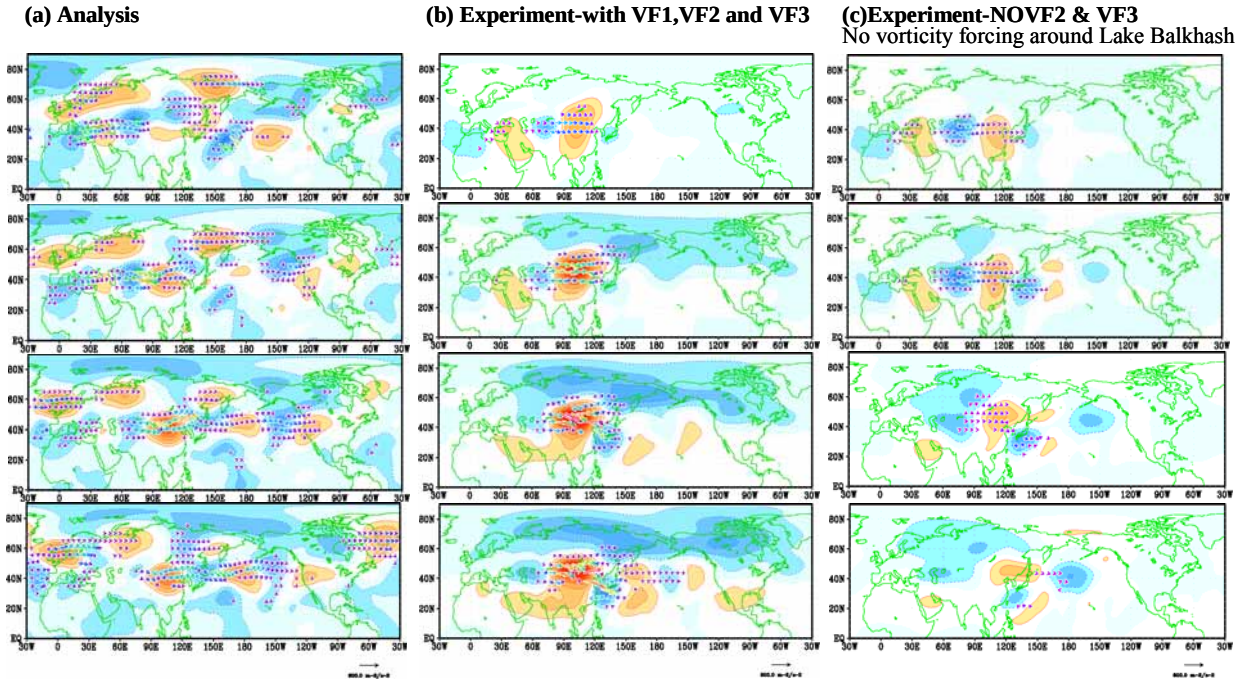

Fig.15 Wave activiy flux and stream function anomaly in Analysis and Experiments.
Contours show stream function anomaly based on the basic flow in an interval of $5x10^6$ m^2 s^{-1}. Red and blue Shadings show anti-cyclonic and cyclonic anomaly, respectively. Vectors show wave activity flux (m^2 s^{-2}). The left panel represents stream function anomaly in the analysis.

4. Summary and conclusion

The features of the large scale atmospheric circulation as a background in the former period of "the extremely heavy rainfall in July 2006" are summarized as follows.

The Baiu front was unprecedentedly active in the former period and brought the extremely heavy rainfall over the wide areas in Japan. There are two reasons why the Baiu front became unprecedentedly active.

One is the large amount of water vapor transport over the East China Sea just before the former period. Typhoon BILIS was moving northwestward from the western Pacific to southern China just before the former period. It is considered that the typhoon strengthened the high pressure over Japan and increased water vapor transport over the East China Sea.

The other is the remarkably strong quasi-stationary Rossby wave packet propagation along the Asian jet. This Rossby wave packet intensified the trough to the north of Japan.

The analysis of Rossby wave sources and results of numerical experiments indicate that the strong wave source around Lake Balkhash amplified the Rossby wave along the Asian jet. It is concluded that the baroclinic eddy to the south of Lake Balkhash had a highly important role in the propagation of the strong Rossby wave from central Asia to Japan.

Reference

Lu, R., and B.J. Kim, 2004: The Climatological Rossby Wave Suorce over the STCZs in the Summer Northern Hemisphere. J. Meteorol. Soc. Jpn., 82, 657–669.

Naoe, H. and Matusda, Y., 1998 : Rossby Wave Propagation and Nonlinear Effects in Zonally-Varying Basic Flows. J. Meteor. Soc. Japan, 76, 385-402.

Onogi, K., J. Tsutsui, H. Koide, M. Sakamoto, S. Kobayashi, H. Hatsushika, T. Matsumoto, N. Yamazaki, H. Kamahori, K. Takahashi, S. Kadokura, K. Wada, K. Kato, R. Oyama, T. Ose, N. Mannoji and R. Taira, 2007 : The JRA-25 Reanalysis. J. Meteorol. Soc. Japan., 85, 369-432.

Takaya, K., and H. Nakamura, 2001 : A Formulation of a Phase-Independent Wave-Activity Flux for Stationary and Migratory Quasigeostrophic Eddies on a Zonally Varying Basic Flow, J.Atom.Sci., 58, 608-627.